OAK RIDGE NATIONAL LABORATORY
operated by
UNION CARBIDE CORPORATION
for the
U.S. ATOMIC ENERGY COMMISSION

ORNL-TM-304

THE PHASE DIAGRAM OF ZIRCONIUM-GALLIUM

D. S. Easton

NOTICE

This document contains information of a preliminary nature and was prepared primarily for internal use at the Oak Ridge National Laboratory. It is subject to revision or correction and therefore does not represent a final report. The information is not to be abstracted, reprinted or otherwise given public dissemination without the approval of the ORNL patent branch, Legal and Information Control Department.

LEGAL NOTICE

This report was prepared as an account of Government sponsored work. Neither the United States, nor the Commission, nor any person acting on behalf of the Commission:

A. Makes any warranty or representation, expressed or implied, with respect to the accuracy, completeness, or usefulness of the information contained in this report, or that the use of any information, apparatus, method, or process disclosed in this report may not infringe privately owned rights; or

B. Assumes any liabilities with respect to the use of, or for damages resulting from the use of any information, apparatus, method, or process disclosed in this report.

As used in the above, "person acting on behalf of the Commission" includes any employee or contractor of the Commission, or employee of such contractor, to the extent that such employee or contractor of the Commission, or employee of such contractor prepares, disseminates, or provides access to, any information pursuant to his employment or contract with the Commission, or his employment with such contractor.

ORNL-TM-304

Contract No. W-7405-eng-26

METALS AND CERAMICS DIVISION

THE PHASE DIAGRAM OF ZIRCONIUM-GALLIUM

D. S. Easton

DATE ISSUED

DEC 12 1962

OAK RIDGE NATIONAL LABORATORY
Oak Ridge, Tennessee
operated by
UNION CARBIDE CORPORATION
for the
U. S. ATOMIC ENERGY COMMISSION

CONTENTS

	Page
ABSTRACT	1
INTRODUCTION	1
MATERIALS	7
EQUIPMENT AND EXPERIMENTAL PROCEDURES	7
Boundary Determination	7
Casting Techniques	14
Annealing Procedures	14
Metallography	17
Alloy Hardness Measurements	27
Preparation and Measurement of X-Ray Specimens	27
DATA AND RESULTS	29
Investigation of the Alpha and Beta Boundaries	29
Intermediate Compounds	35
Lattice Parameter Measurements	35
SUMMARY AND CONCLUSIONS	37
ACKNOWLEDGMENT	40
APPENDIX	41

THE PHASE DIAGRAM OF ZIRCONIUM-GALLIUM

D. S. Easton

ABSTRACT

The zirconium-rich portion of the zirconium-gallium phase diagram was determined by the examination of microstructures of isothermally annealed and quenched alloys. In order to maintain the highest possible purity level of the constituents, control of all phases of the investigation was given careful consideration. Although the purity of the alloys was at least 99.9%, a deviation from binary equilibrium was observed in the region between the alpha and beta phases.

As a result of the large difference in atomic size between zirconium and gallium, the slopes of the alpha-beta boundaries were depressed and the solubility of the solid solution phases were restricted when compared to the addition of other Group IIIB elements. The a_o and c_o lattice constants of close-packed hexagonal zirconium were contracted and the axial ratio was expanded by the addition of gallium. The change in c/a was very close to the change observed in zirconium-indium alloys, implying that the size misfit had little effect on the axial ratio.

A eutectoid reaction occurred at 860°C with beta solid solution (1.8 at. % Ga), decomposing into alpha solid solution (0.8 at. % Ga) and Zr_3Ga. On the basis of cast microstructures, a eutectic reaction occurs in which liquid (~ 21.0 at. % Ga) decomposes into beta (~ 8.0 at. % Ga) and Zr_5Ga_3. It is proposed that intermediate phases are formed at 25.0 at. % Ga (Zr_3Ga), 37.5 at. % Ga (Zr_5Ga_3), and 50.0 at. % Ga (ZrGa).

INTRODUCTION

The study of the system, zirconium-gallium, is an extension of a study of a series of zirconium-phase diagrams chosen to show the effects of solutes of different valencies and atomic size. Figure 1 shows phase diagrams of zirconium with various solutes and the atomic size differences

UNCLASSIFIED
ORNL-LR-DWG 70693R

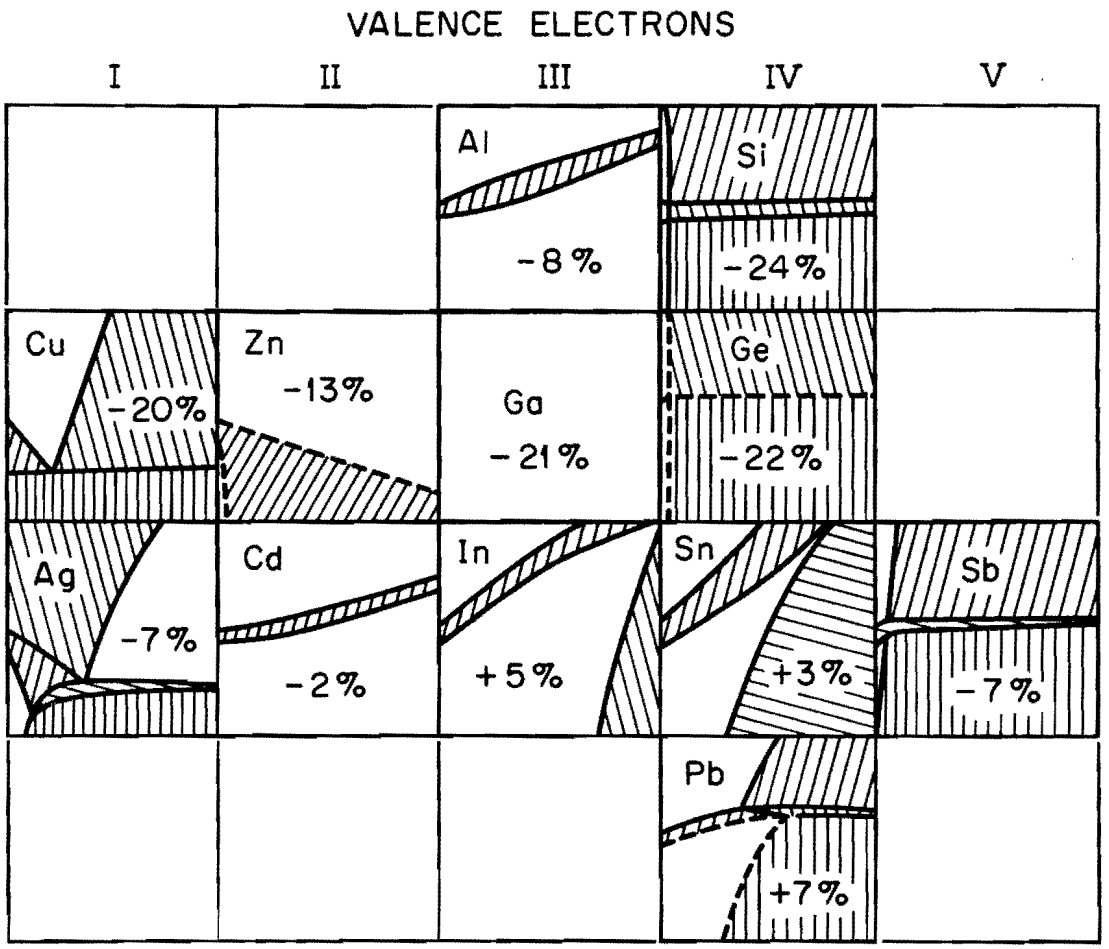

Fig. 1. Phase Diagrams of Zirconium with Various Solutes in the Composition 0–10 at. % Solute and Temperature Range of 775–975°C. Atomic size differences $\left(\frac{d_{solute} - d_{Zr}}{d_{Zr}} \times 100\right)$ are indicated by numbers within blocks.

for the solutes. The desirability of establishing the zirconium-gallium phase diagram is apparent.

A literature survey revealed no information on the zirconium-rich region with which this study is primarily concerned. Anderko[1] reported an intermediate phase of approximately 25 at. % Ga (Zr_3Ga) and a peritectically formed phase at 37.5 at. % Ga (Zr_5Ga_3). The Zr_5Ga_3 phase was found to be an ordered hexagonal structure, but the exact composition and structure of the Zr_3Ga phase was not determined. H. J. Wallbaum[2] found a compound, $ZrGa_3$, which had a tetragonal structure and was analogous to that found in the titanium-gallium system.

Interest in zirconium and zirconium alloys was intensified when it first became feasible to separate hafnium from zirconium in the early 1950's. The low cross-section absorption (< 0.20 barn)[3] of zirconium made its use as a reactor material important, and its resistance to corrosion[4] and generally good mechanical properties[5] made it desirable for other applications as well.

Zirconium is a Group IVA transition element with two 4d and two 5s electrons in the outer shells. It exists in two allotropic forms, alpha (close-packed hexagonal) and beta (body-centered cubic) with the transformation occurring at 864.5 ± 7.5°C. The cubic structure cannot be retained on cooling unless substantial amounts of alloying elements are added. Using a hard sphere approximation,[6] the closest distance of

---

[1]K. Anderko, Z. Metallk. 49, 165 (1958).

[2]H. J. Wallbaum, Z. Metallk. 34, 118 (1942).

[3]Neutron Cross Sections: A Compilation of the AEC Neutron Cross Section Advisory Group, Report AECU-2040, Supplement 3, April 1, 1954.

[4]G. L. Miller, Zirconium, p. 203, Butterworths Scientific Publication, London, 1954.

[5]Ibid., pp. 130–143.

[6]W. Hume-Rothery and G. V. Raynor, The Structure of Metals and Alloys, pp. 60–96, Institute of Metals, 1956.

approach of the atoms in the hexagonal is 3.179 A and in the cubic (corrected to 25°C) is 3.10 A. In choosing zirconium as the base solvent in a study of the theory of alloying, there was therefore a combination of both fundamental and practical interest.

Gallium is a Group IIIB element with two 4s and one 4p electrons in the outer shells. It has an unusual orthorhombic structure with each atom having six neighbors at an average distance of 2.75 A and one neighbor at 2.44 A. Table 1 shows some physical properties of zirconium and gallium.

The metallic valency of transition elements, such as zirconium, is not clearly defined and changes in the phase diagrams of various zirconium systems might permit a more exact determination of the number of effective valence electrons.

Betterton and Frye[7] have shown that, when the variation of the temperature of the alpha-beta boundaries of various solutes is plotted against the electron concentration, the resulting curve is linear. They also suggested that, although zirconium is tetravalent in the free ion, a change in the sign of the slope of the alpha-beta boundaries between elements of univalency and trivalency indicates that it should be considered divalent. This change of slope of the alpha-beta boundaries of zirconium with solutes of varying valencies of the fifth period is shown in Fig. 2.

Phase diagrams of other systems were found to be affected by the number of valence electrons in the solutes in a study conducted by Hume-Rothery et al.[8] Hume-Rothery has also shown that, in general, when two elements are considered the one of lower valency will be less soluble in the higher valence element than vice versa. In regards to atomic size, he hypothesized that if the size of the atoms of the solute

---

[7]J. O. Betterton, Jr., and J. H Frye, Jr., Acta Met. 6, 205 (1958).

[8]W. Hume-Rothery, G. W. Mabbot, and K. M. Channel-Evens, Phil. Trans. Roy. Soc. London, Ser. A 233, 1 (1934).

Table 1. Selected Physical Properties of Zirconium and Gallium

Symbol	Zr	Ga
Atomic Number	40	31
Atomic Weight	91.22	69.72
Density, g/cm^3	6.5	5.91
Melting Point, °C	1852 ± 10	29.78
Boiling Point, °C	~3700	2070
Crystal Structure	hcp <865°C bcc >865°C	Orthorhombic
Lattice Constants, A	a = 3.2326 c = 5.1473 c/a = 1.5923	a = 4.5258 b = 4.5198 c = 7.6602
Closest Distance of Approach, A	3.1	2.44
$\frac{d_{Ga}-d_{Zr}}{d_{Zr}} \times 100$	∞	−21%
Cross Section Absorption (barns)	<0.2	3.3
Specific Heat at 20°C cal/g-°C	0.066	0.079

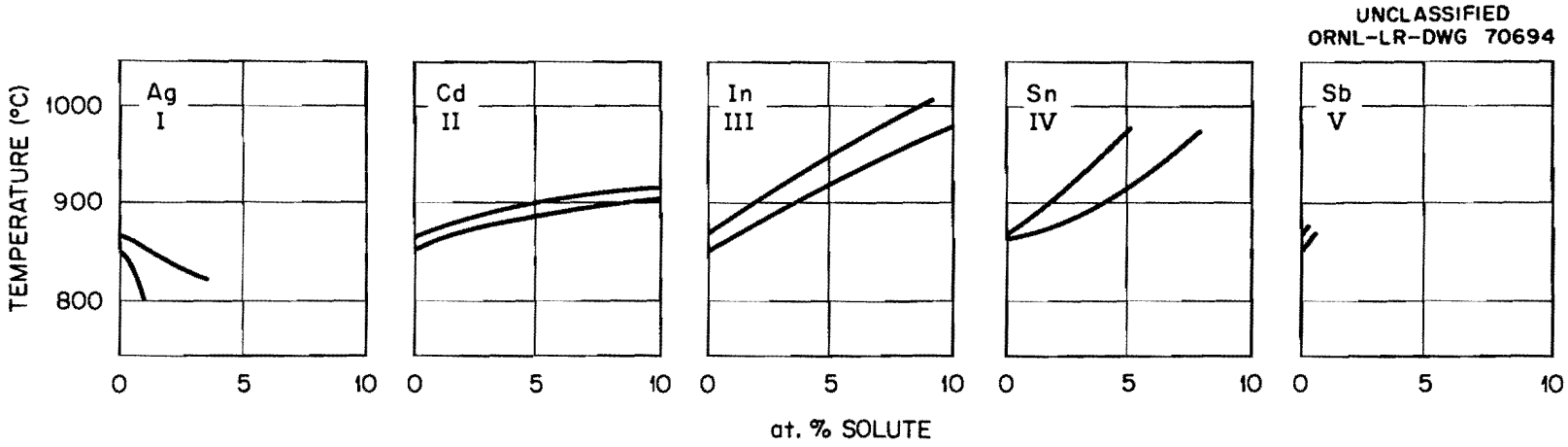

Fig. 2. A Comparison of the Alpha-Beta Boundaries of Zirconium with Solutes of Various Valency.

and solvent differ by more than 15%, the solubility will be restricted.[9] Extensive solid solubility might be expected for size factors of less than this amount.

Except for the size factor effect, gallium would be expected to behave much like other Group IIIB elements, aluminum and indium, which, along with a reasonably large solubility in zirconium, have alpha-beta boundaries with positive slopes. Figure 3 shows the phase diagrams of zirconium-indium, zirconium-aluminum, and the status of zirconium-gallium prior to this report and including work by Anderko[1] reported after the start of this project.

MATERIALS

Two 20-g lots of gallium, one containing < 10 ppm impurities and the other < 3 ppm impurities by spectrographic analysis, were obtained from the Jarrell-Ash Company, Newtonville, Massachusetts. Westinghouse Grade I iodide-zirconium with a purity of 99.95% was employed as the base solvent. A particular bar was selected on the basis of impurity analysis and was used throughout the experiment. Table 2 shows the minor impurity analysis of both the original zirconium, gallium, and the final alloys. Substantially no increase in impurity level was found in the final alloys when compared to the original material.

EQUIPMENT AND EXPERIMENTAL PROCEDURES

Boundary Determination

The method of microscopic examination of isothermally annealed and ice-quenched alloys was chosen to determine boundary positions. The sensitivity of the experimental method is illustrated by the microstructures, Figs. 4–7, of four alloys annealed at 843°C. Although

---

[9]W. Hume-Rothery and G. V. Raynor, The Structure of Metals and Alloys, pp. 108–9, Institute of Metals, 1956.

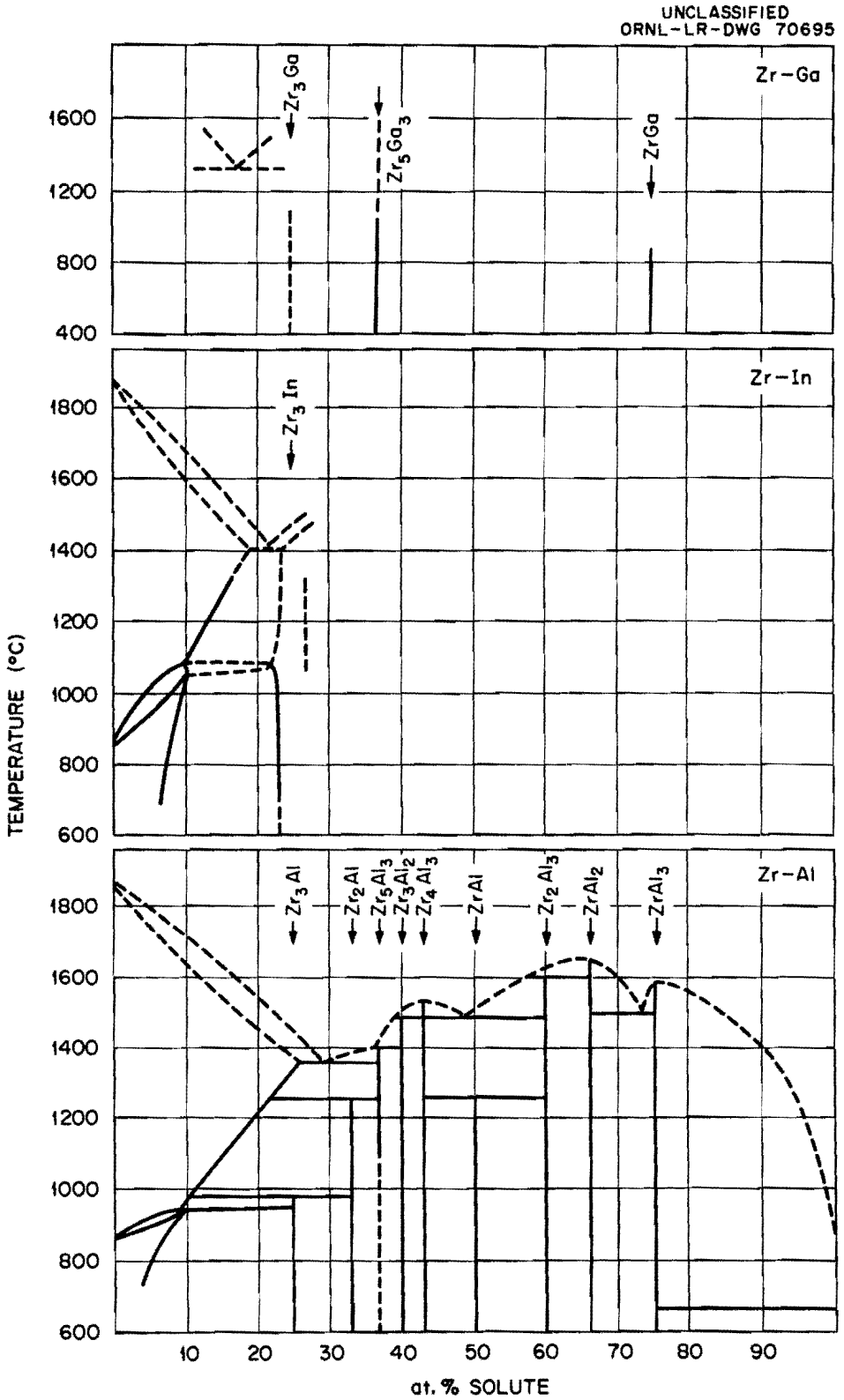

Fig. 3. Comparison of the Phase Diagrams of Zr-Al, Zr-In, and the Previously Existing Diagram of ZrGa.

Table 2. Minor Impurities

Material	Neutron Activation Analyses (ppm)								Vacuum Fusion (ppm)		
	Cu	Cr	Ta	Mo	Fe	W	Si	Ni	H_2	O_2	N_2
Bar zirconium (degassed)	0.47	3.9	56	1.7	23.3	0.2	5.0	11.9	<1.0	17	<5.0
	0.45		107	1.1	28		2.2	16.9	3.0	20	<5.0
	0.47	<15	123	1.1	30	<0.01	5.5	12.1	2.0	22	<5.0
	0.79										
Zr-Ga alloys	4.5	0.90	<0.01	0.64	39	3.4		5.0	3	20	<5
	3.9	0.83	0.01	0.58	47	3.1		6.0	3	21	<5
	9.2	0.12	0.02	1.69		13.2					
	8.7	1.5		1.60		6.6			4	33	<5
	2.3					0.058					
	1.1					0.055					

Spectrographic Analyses

	Cu	Pb	Sn	Ca	Ag	Mg
Gallium	5	2	2	<1	<1	
	1	<1			1	<1

Elements sought but not detected: Al, As, Au, B, Ba, Be, Bi, Cd, Co, Cr, Cs, Fe, Ge, Hf, Hg, In, Ir, K, Li, Mg, Mn, Mo, Na, Nb, Ni, Os, P, Pd, Pt, Rb, Re, Rh, Ru, Sb, Se, Si, Sr, Ta, Te, Ti, Tl, V, W, Zn, Zr

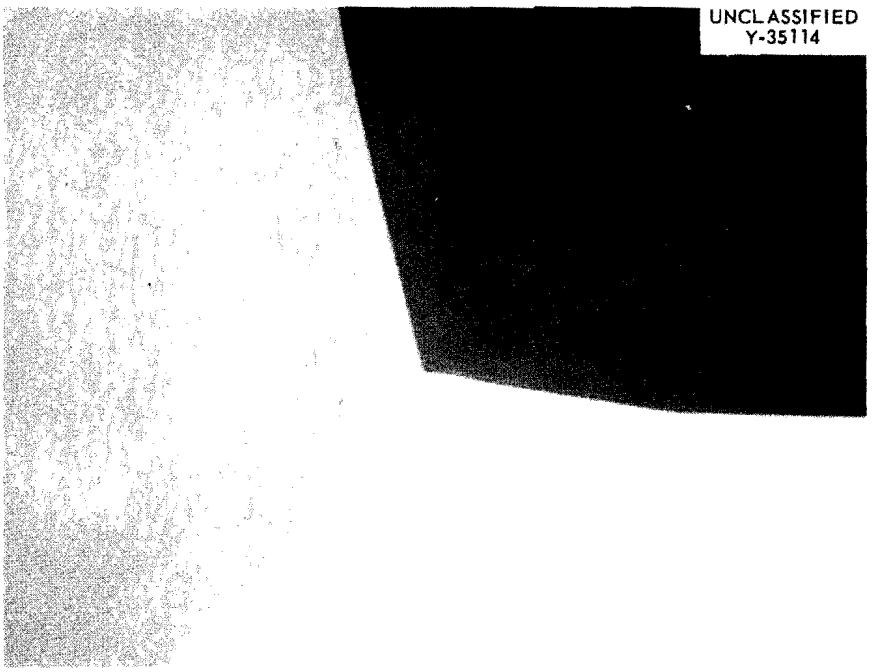

Fig. 4. Zirconium–0.5 at. % Ga Alloy in the Homogeneous Alpha Phase Region After Annealing at 843°C. Etchant: HNO_3-H_2O-HF. 500X.

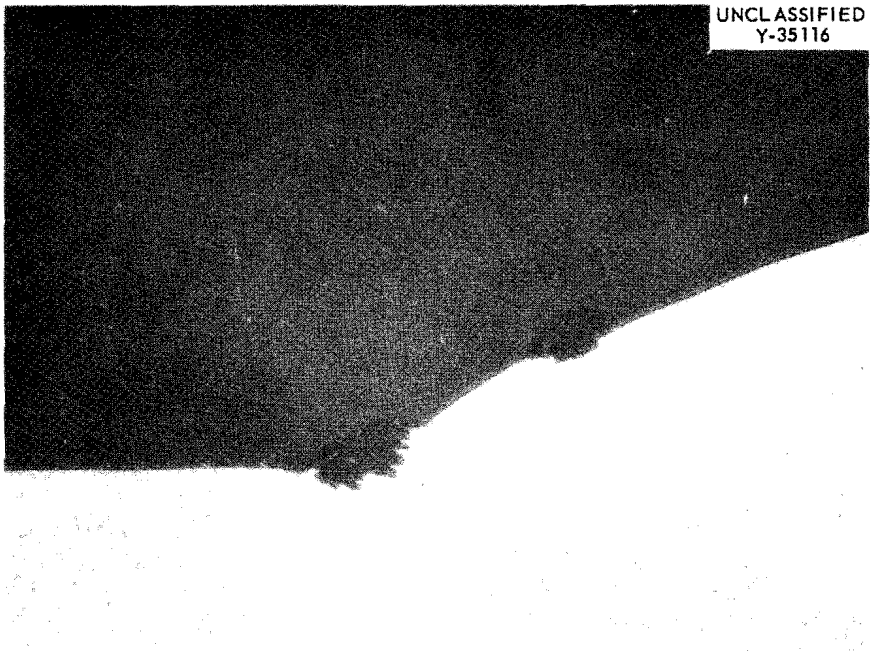

Fig. 5. Zirconium-0.8 at. % Ga Alloy Showing Two Grains of Transformed Beta in an Alpha-Phase Grain Boundary After Annealing at 843°C. Etchant: HNO_3-H_2O-HF. 500X.

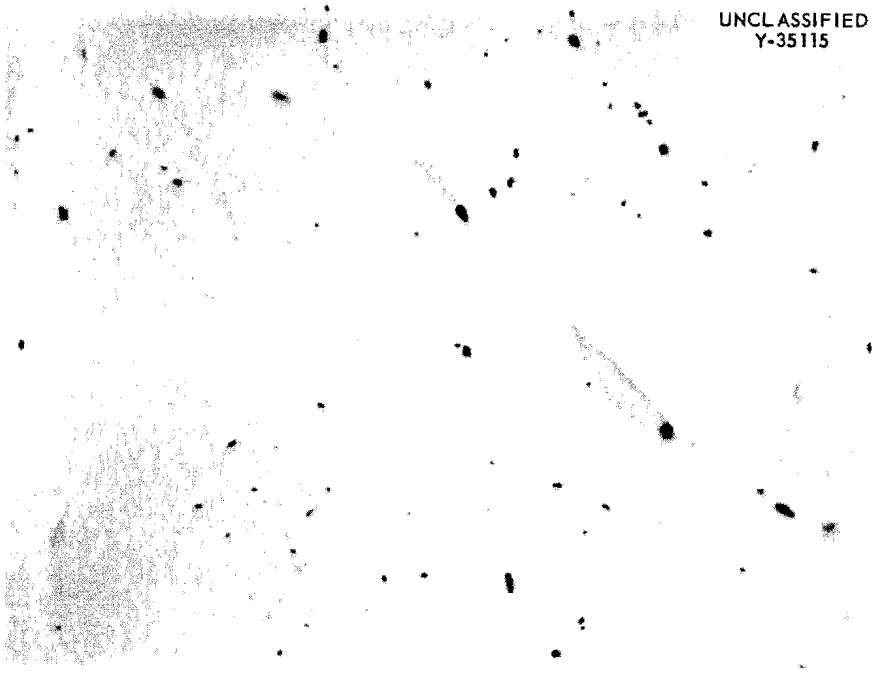

Fig. 6. Zirconium-1.1 at. % Ga Alloy with a Matrix of Alpha Phase Containing Small, Dark Gamma Crystals (Zr_3Ga) and Transformed Beta (Gray Areas in Grain Boundary). Annealed at 843°C.
Etchant: HNO_3-H_2O-HF. 500X.

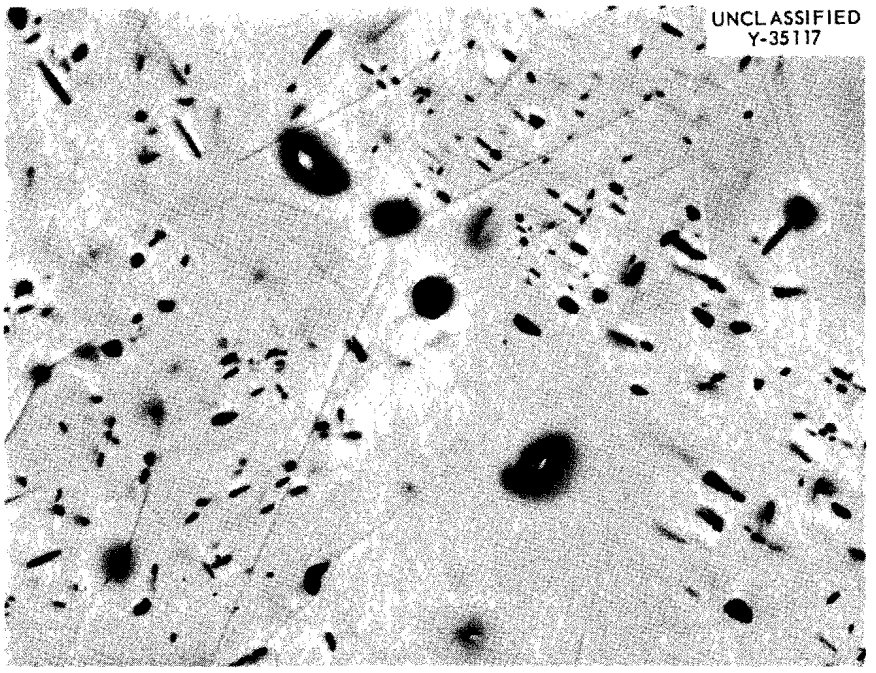

Fig. 7. Zirconium–1.3 at. % Ga Alloy in the ($\alpha + \gamma$) Region After Annealing at 843°C. Etchant: HNO_3-H_2O-HF. 500X.

separated by approximately 0.3 at. % Ga, they represent regions comprised of alpha, alpha plus beta, alpha plus beta plus compound, and alpha plus compound, respectively. Each alloy was examined on two or more sections before being submitted to the Johnson, Matthey and Company, Limited, Wembley, Middlesex, England, for determination of the amount of the solute present.

The volume percent of phases present in the microstructures were measured using an integrating stage mounted on a metallograph. Figure 8 shows the volume percent of gamma phase present in a series of alloys annealed at 1095°C in the beta plus gamma region. The extrapolation of this curve places the beta boundary at 4.5 at. % Ga and the gamma boundary at 27 at. % Ga.

Casting Techniques

Specimens were prepared by melting approximately 10-g ingots in an arc furnace, shown in Fig. 9, which consisted of a water-cooled copper hearth and a water-cooled tungsten electrode. The system was first purged by evacuating to pressures of less than 1×10^{-7} mm Hg and then filled with pure argon for arc stability. The leak rate of the system when blanked off was on the order of 2×10^{-7} mm Hg/min. Although gallium has a melting point of only 29.8°C, the boiling point is 2070°C and no difficulty was experienced with vaporization loss during casting. Each alloy, along with a getter of pure zirconium, was cast six times and the ingot inverted after each casting. The hardness increase, which is an indication of purity, was less than 1 VHN/casting in pure zirconium samples.

Annealing Procedures

The cast ingots were cold worked to the extent that the composition permitted, filed, etched, and wrapped first in zirconium and then in molybdenum foil. The molybdenum prevented the reaction between the

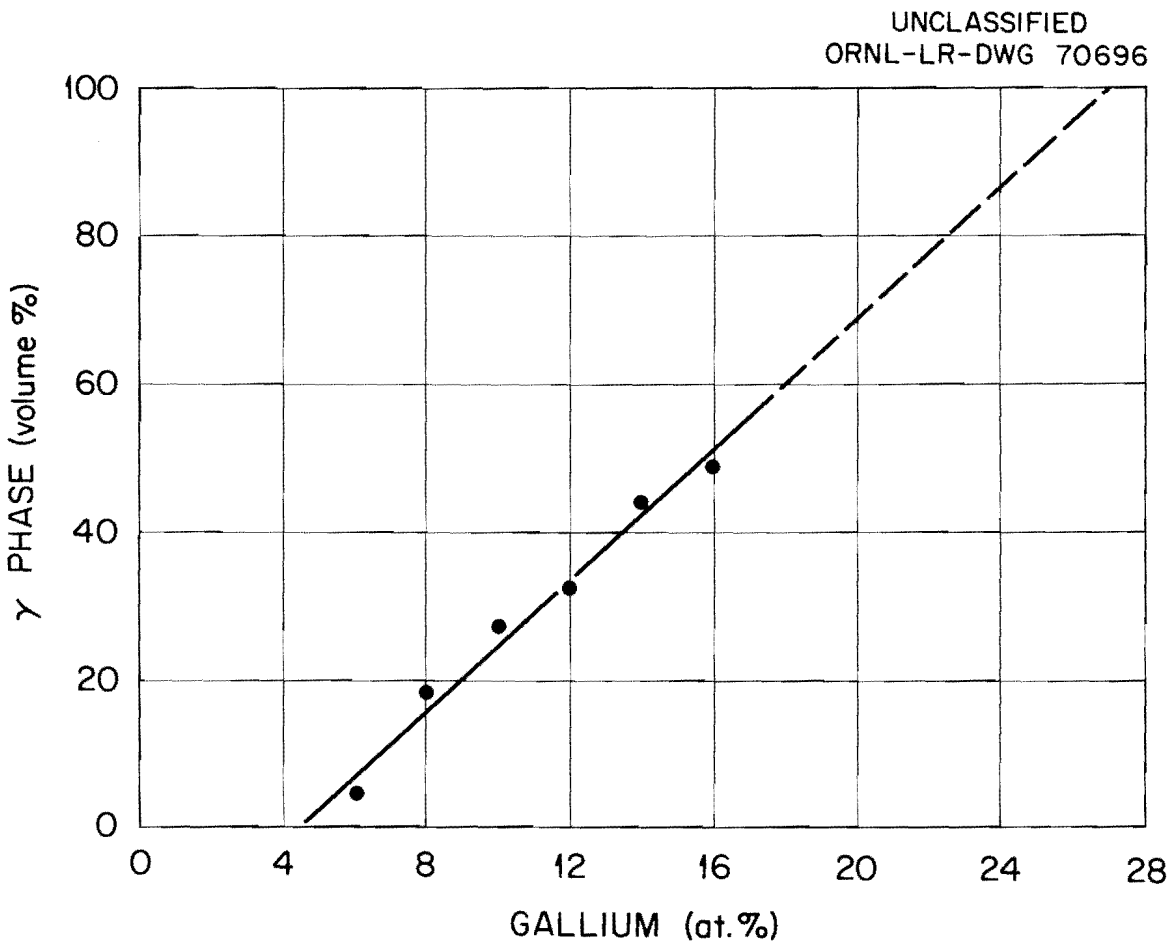

Fig. 8. The Volume Percent of Compound Present in a Series of Zirconium-Gallium Alloys Annealed at 1095°C.

UNCLASSIFIED
Y-34963

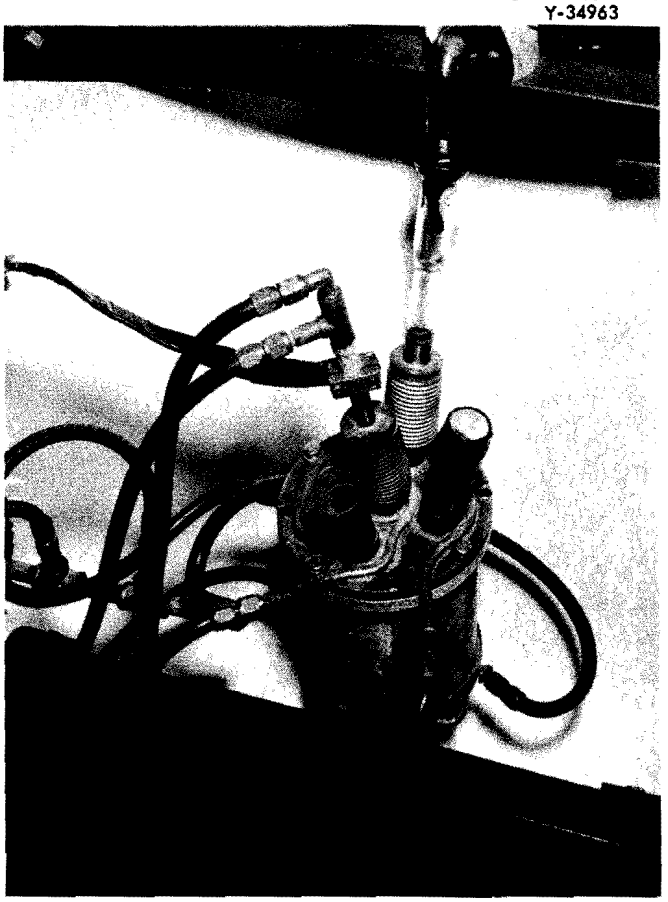

Fig. 9. Arc Casting Furnace.

zirconium and the quartz capsule, and the zirconium foil protected the specimen from the molybdenum. The specimens were placed in individual quartz tubes, vacuum degassed to remove hydrogen at the temperatures at which the anneal was to take place, filled with a partial pressure of pure argon, and sealed in capsule form. Each alloy had an initial heat treatment of 10 days at 1100°C to remove inhomogeneities resulting from casting. Specimens of pure zirconium, cast and annealed in the same manner as the alloys, showed no hardness increase due to this procedure. After annealing times ranging from 65 days at 750°C to 2 days at 1250°C, the samples were rapidly quenched in ice water.

Temperature variations were held to less than 1°C for the period of the anneal. Figure 10 shows the temperature variation of a typical anneal covering a period of 48 days. Temperatures were measured by Pt_{90} Rh_{10}-Pt thermocouples which were frequently calibrated against the melting points of high-purity palladium, gold, silver, aluminum, zinc, tin, and ice. Typical calibration curves of a single thermocouple and covering a period of 14 months are shown in Fig. 11. All sample temperatures were corrected to an extrapolated change between calibrations.

The alpha-beta transformation temperature range of pure zirconium has been measured repeatedly for a number of years in this laboratory. It is an indication of the extremely close control of factors such as base purity, casting, annealing, and temperature measurement that the temperature range of the transformation has always occurred during this time period uniformly between 857 ± 3°C and 872 ± 1°C.

Metallography

After quenching, the samples were mounted in bakelite, polished, and etched with variations of a 46 HNO_3–46 H_2O–8 HF etchant. Examination was carried out on a Bausch and Lomb metallograph at various magnifications to determine the structures present. Since the beta phase could not be retained, grains of prior beta were recognized by their transformation structure. In alloys up to approximately 1.0 at. % Ga, the prior beta grains had serrated boundaries while above that composition they appeared

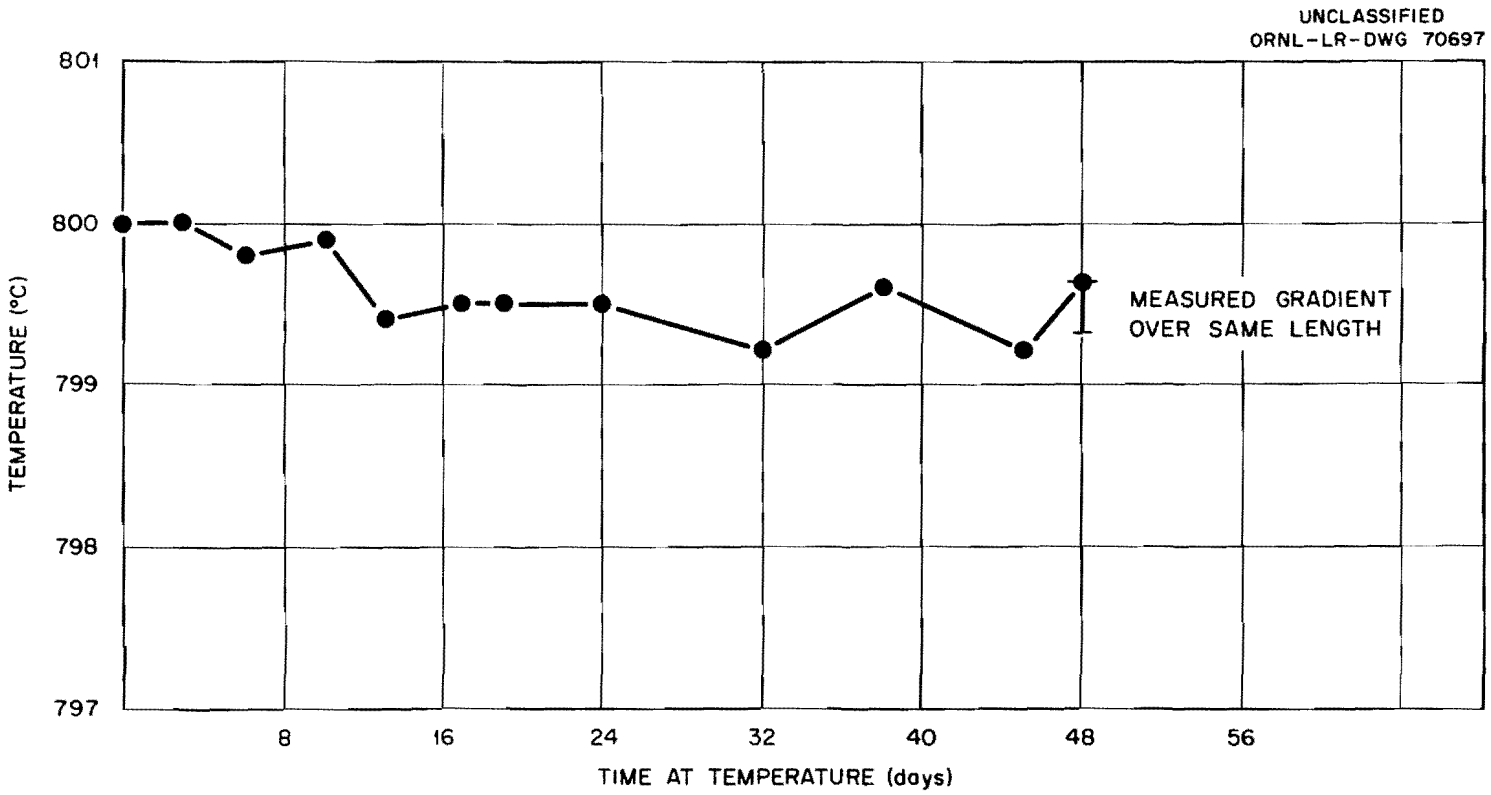

Fig. 10. Temperature Record of a Typical Anneal Held 48 Days at 799.6 ± 0.4°C.

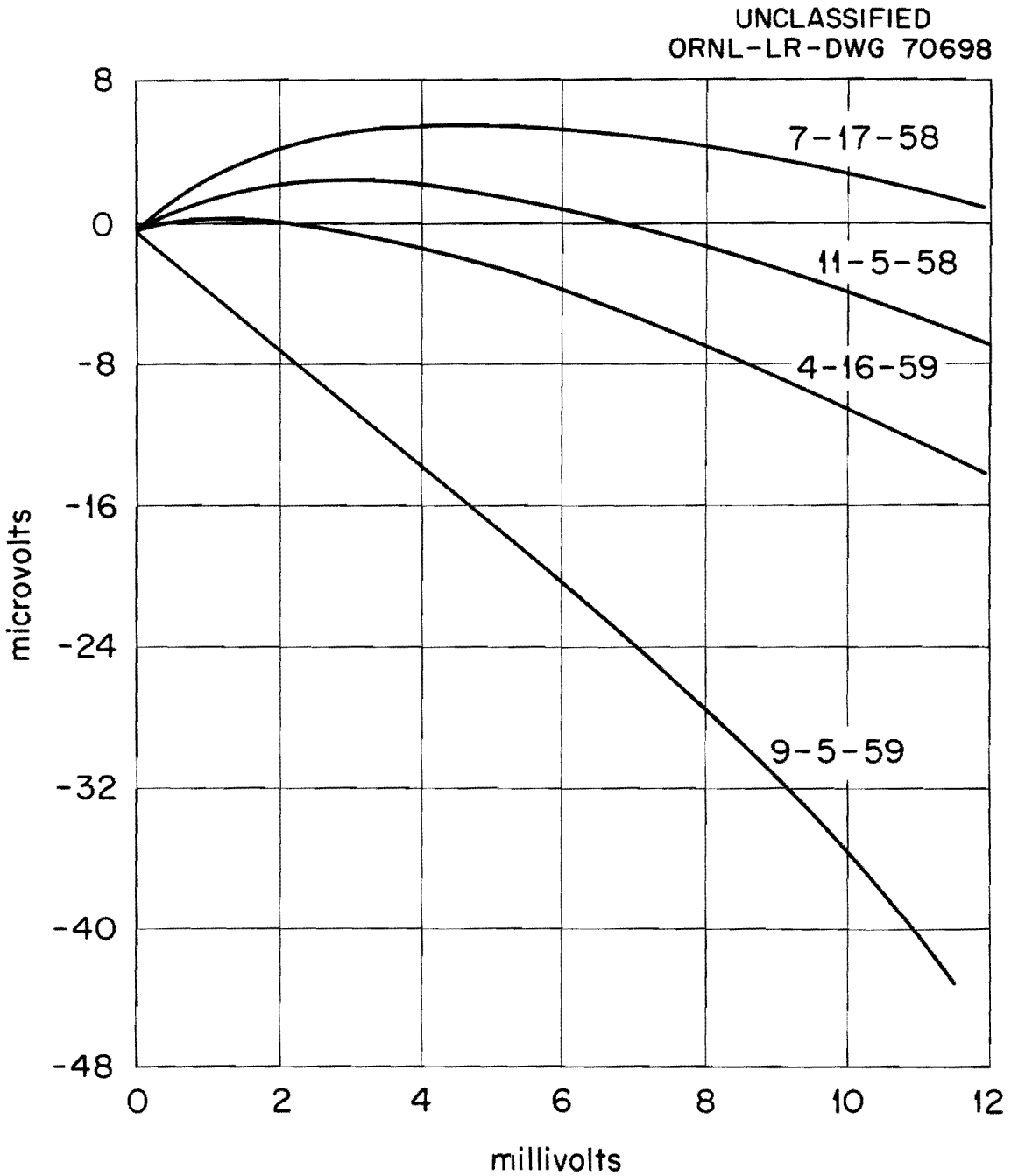

Fig. 11. Calibration Curves of a Pt vs Pt–10% Rh Thermocouple Showing Deviation from the 1948 International Tables.

as "basketweave" or a martensitic-type structure closely resembling that found in the Fe-Fe_3C system. The alpha grains had smooth isothermal grain boundaries. In the alpha plus compound regions, annealing times long enough to permit coalescence to large compound grains were prohibitive, and therefore the compound appeared as very small particles which because of their extreme hardness and reactivity with etching reagents were hard to resolve. In the beta plus compound region the compound formed large angular grains which could be brought out in the microstructure more easily. Typical microstructures are shown in Figs. 12–17.

Figure 12 shows pure zirconium in the homogeneous alpha phase region after annealing at 859.3 ± 0.3°C for 35 days. The smooth grain boundaries are typical of the grains that did not undergo the alpha-beta transformation. Figure 13 shows a Zr–0.68 at. % Ga alloy in the homogeneous beta phase region after annealing at 871.3 ± 0.6°C for 45 days. The serrated grain boundaries indicate the transformation that has taken place. The specimen is called beta although at room temperature it has a close-packed hexagonal or alpha structure. Figure 14 shows a Zr–1.24 at. % Ga alloy in the homogeneous beta phase region after annealing at 866.0 ± 0.3°C for 24 days. This microstructure illustrates the "basketweave" or martensite-type transformation structure. At the temperature of the anneal the structure was body-centered cubic. Figure 15 shows a Zr–0.8 at. % Ga alloy in the alpha plus beta phase region after annealing at 866.0 ± 0.3°C for 24 days. This microstructure shows an unusual occurrence of a twin apparently extending through the grain boundaries of two different phases. The alpha grains are the light colored grains with smooth boundaries. The orientation of the crystals were apparently very close. Figure 16 illustrates a Zr–2.4 at. % Ga alloy in the beta plus compound region after annealing at 900.0 ± 0.3°C for 22 days. The angular grains are Zr_3Ga crystals in a matrix of prior beta. Figure 17 shows Zr–12.0 at. % Ga alloy in the as-cast condition. Because of severe pitting during etching the microstructure is shown in the as-polished condition. A eutectic structure of beta plus gamma along with primary grains of beta is shown.

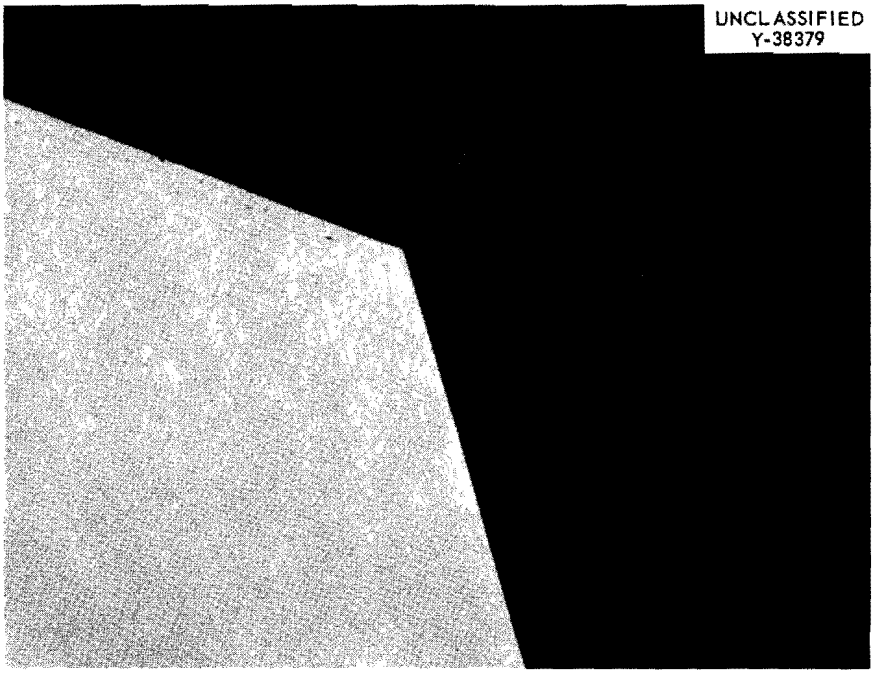

Fig. 12. Pure Zirconium in the Homogeneous Alpha Phase Region After Annealing at 859.3°C. Etchant: HNO_3-H_2O-HF. 500X.

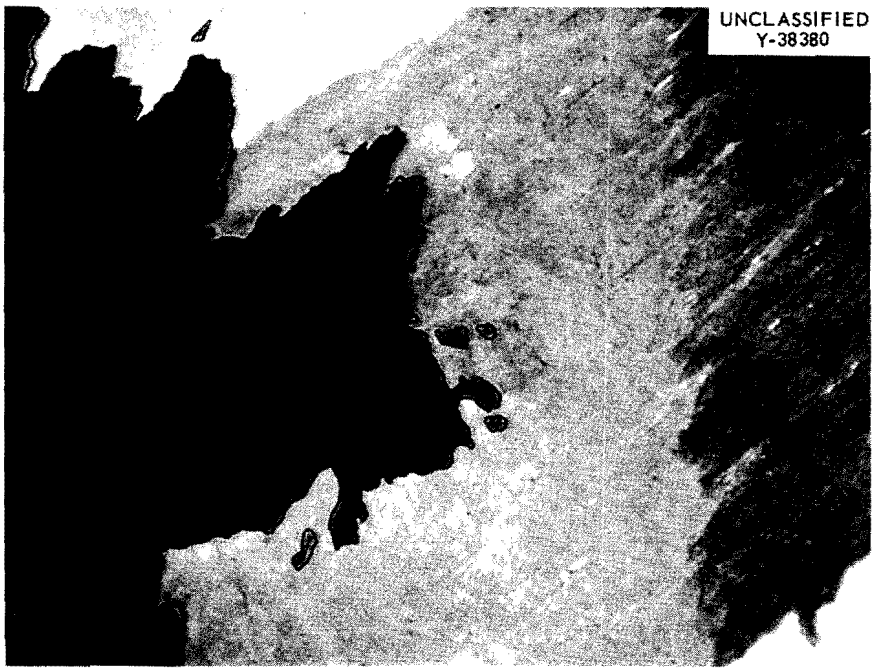

Fig. 13. Zirconium–0.68 at. % Ga Alloy in the Homogeneous Beta Phase Region After Annealing at 871.3°C. Etchant: HNO_3-H_2O-HF. 500X.

Fig. 14. Zirconium–1.24 at. % Ga Alloy in the Homogeneous Beta Phase Region After Annealing at 866°C. Etchant: HNO_3-H_2O-HF. 250X.

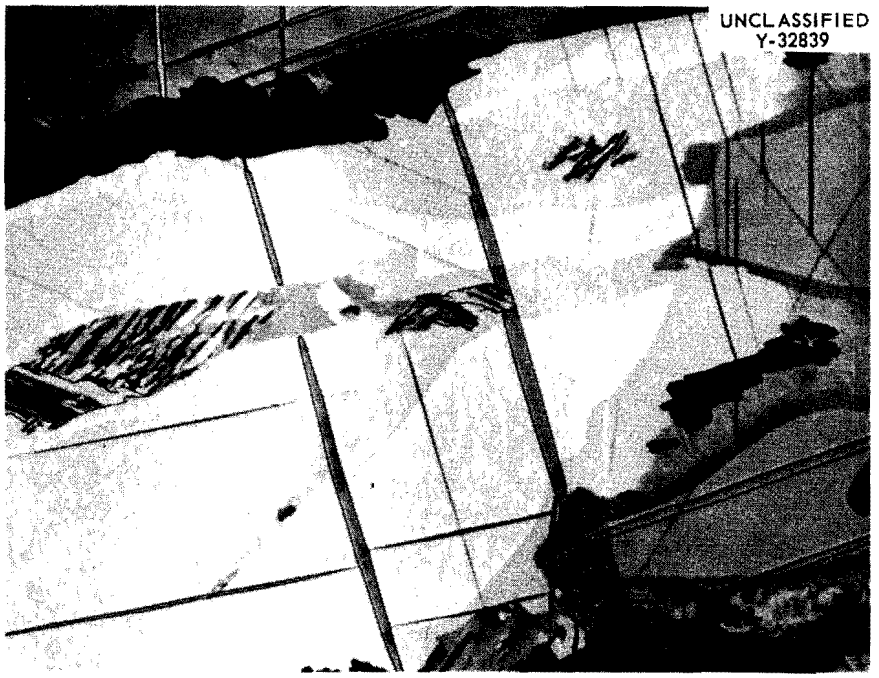

Fig. 15. Zirconium–0.8 at. % Ga Alloy in the $\alpha + \beta$ Phase Region After Annealing at 866°C. Etchant: HNO_3-H_2O-HF. 250X.

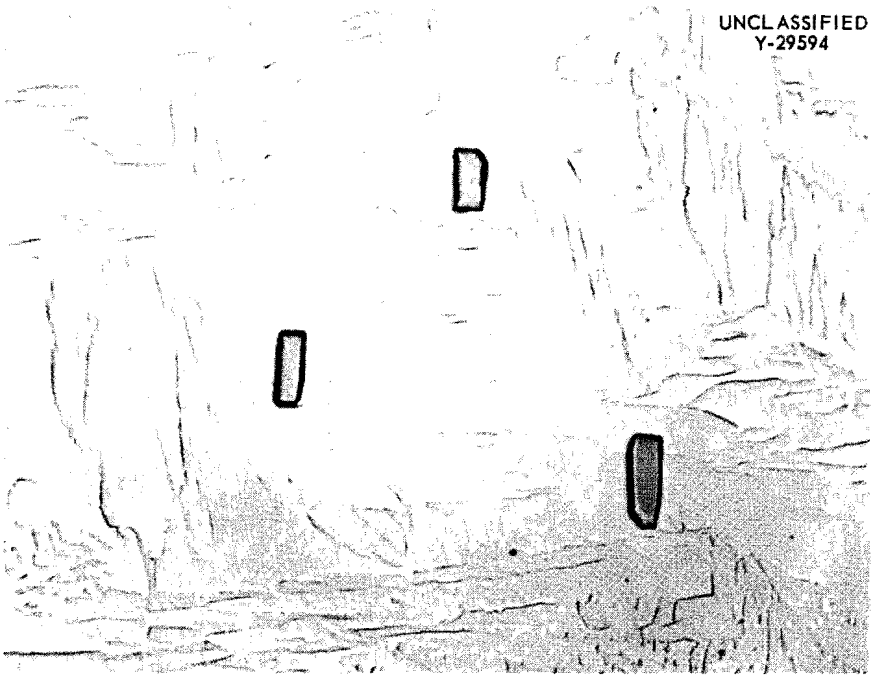

Fig. 16. Zirconium–2.4 at. % Ga Alloy with a ($\beta + \gamma$) Microstructure After Annealing at 900°C. Etchant: HNO_3-H_2O-HF. 500X.

Fig. 17. Zirconium-12.0 at. % Ga Alloy in the As-Cast Condition. As-polished. 2000X reduced 2%.

Alloy Hardness Measurements

Hardness values were used as an indication of control of impurity level. The measurements were made on a Vickers hardness machine using a 10-kg load. Five impressions were made on each sample. Figure 18 shows a plot of VHN vs composition for specimens quenched from various temperatures.

Preparation and Measurement of X-Ray Specimens

Samples to be used for x-ray measurements were annealed in the described manner in bulk form and the alpha microstructure confirmed. Following this they were swaged into wire of 0.048-in. diam, the surface filed and etched, and given a final anneal of 3 min in the alpha region to remove the cold-worked structure. The vacuum system used for the final anneal could be evacuated to 2×10^{-10} mm Hg cold- and approximately 5×10^{-8} mm Hg at the alpha-annealing temperature. The specimens were then etched to less than 0.010-in. diam for the x-ray measurement. Pure zirconium samples treated in this fashion showed no difference in lattice parameters between etched and unetched specimens. Exposures were made in a 11.43-cm Debye-Scherrer camera with temperatures held to 19 ± 1°C. Unfiltered copper radiation of the following wavelengths was used $\lambda\alpha_1 = 1.54050$, $\lambda\alpha_2 = 1.54434$, and $\lambda\beta_1 = 1.39217$. The films were measured on a Gaertner comparator to the nearest thousandths of a millimeter.

The a_i parameter was obtained from the formula,

$$a_i^2 = \frac{4/3(h^2 + k^2 + hk) + \ell^2(c/a)^2}{\sin^2\theta/(\lambda/2)^2} .$$

The points were then plotted using a Nelson-Riley[10] graphical extrapolation function which corrects for absorption. A c/a ratio was first approximated

[10] J. B. Nelson and D. P. Riley, Proc. Phys. Soc. (London) 57, 160 (1945).

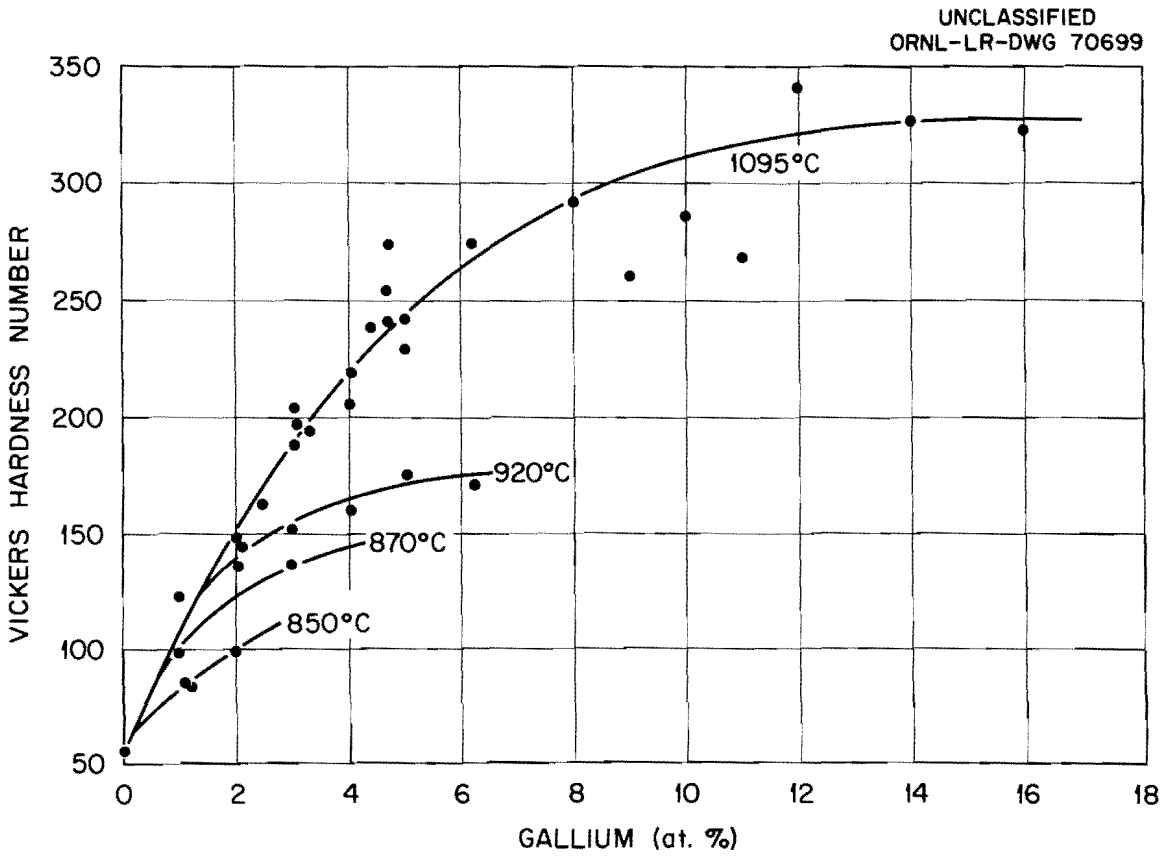

Fig. 18. Hardness Curves of Alloys Quenched from Various Temperatures.

and then adjusted to minimize the scatter in the values of the "a_i" dependent and the "c_i" dependent lines from a common straight line. Two approximations usually were necessary in order to make the points approach a single curve. A typical extrapolation curve is shown in Fig. 19.

DATA AND RESULTS

Investigation of the Alpha and Beta Boundaries

The diagram as experimentally determined is very similar to that of the Fe-Fe_3C diagram, which includes a eutectic and eutectoid reaction. A partial diagram of the eutectoid region, as determined experimentally, is shown in Fig. 20. A table of data containing annealing information, composition, hardness, and observed microstructures is given in the Appendix.

A eutectoid reaction, β(1.8 at. % Ga) $\leftrightarrows$ α(0.8 at. % Ga) + γ(25.0 at. % Ga), was found to occur at 860°C. The maximum solubility of the alpha phase was 0.8 at. % Ga.

The alpha-beta transformation of the base zirconium occurs over a range of temperatures between 857 ± 3°C and 872 ± 1°C. This separation, due to minor impurities along with the separation of the horizontal boundaries of the diagram into temperature bands, makes the determination of a truly binary system unattainable. This situation may be visualized by assuming an impurity (iron)[11] which has a very restricted alpha solubility and a lower eutectoid temperature than that of gallium and by taking a vertical section from a zirconium-gallium impurity diagram. If one assumes that the major impurities are of this eutectoid forming type, then the alpha-alpha plus beta boundary would be rotated upward and both the transformation and eutectoid temperatures would be increased slightly. The diagram can thus be idealized as in Fig. 21. If the major

---

[11]E. T. Hayes, A. H. Roberson, and W. L. O'Brien, Trans. ASM 43, 888–904 (1951).

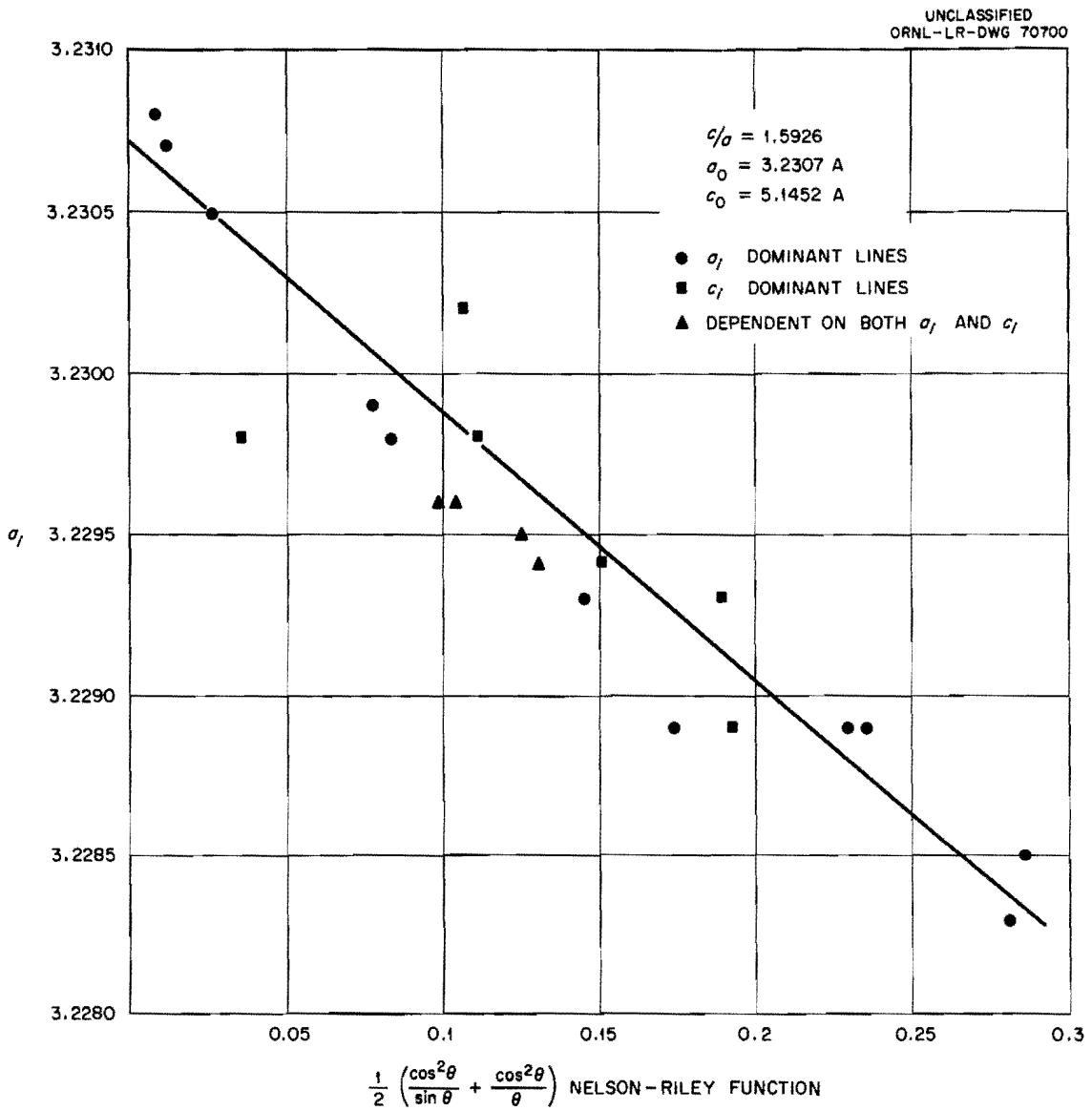

Fig. 19. Graphical Extrapolation of X-Ray Data on an 0.3 at. % Ga Alloy.

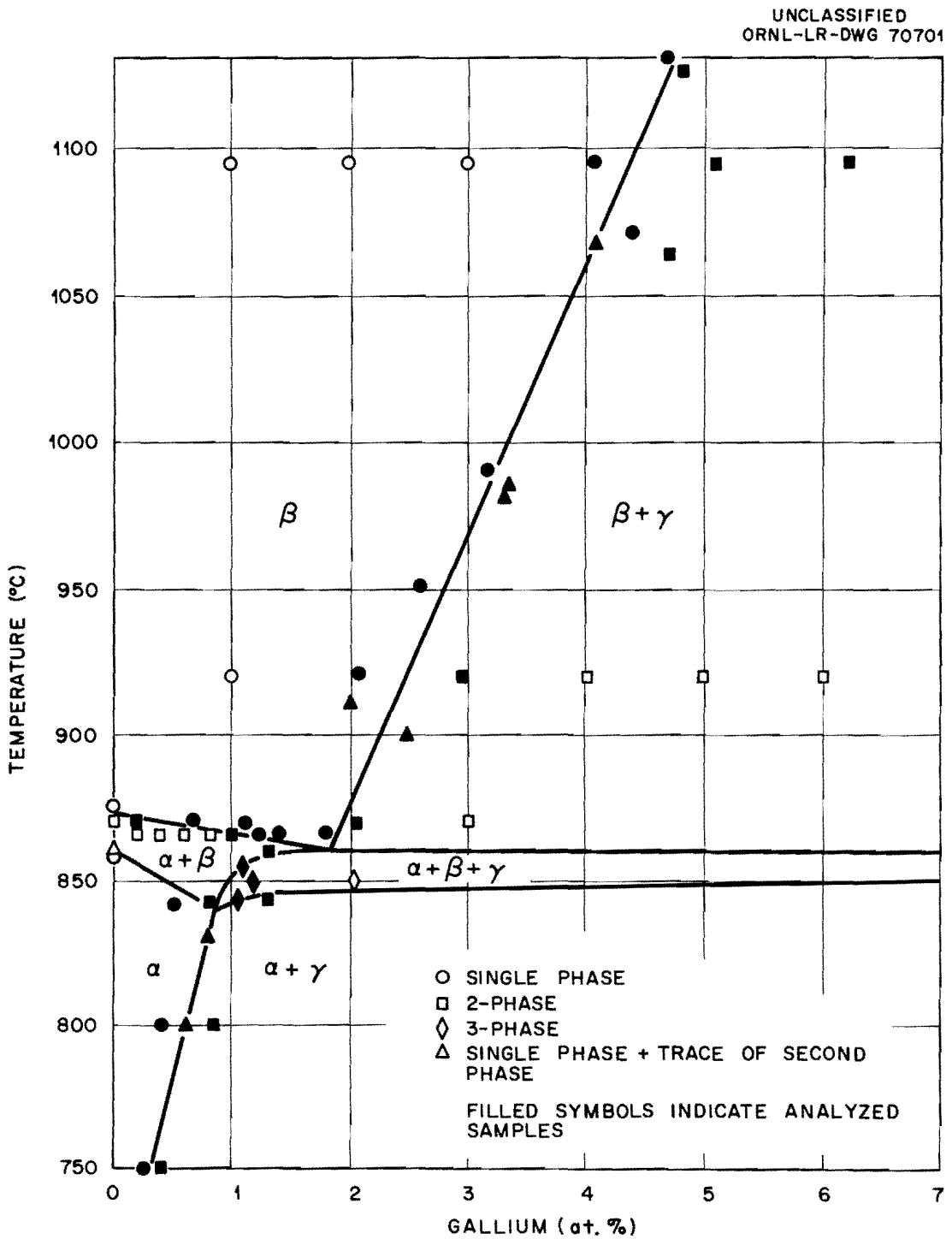

Fig. 20. Experimental Diagram of the Zr-Ga Eutectoid Region Showing Deviation from True Binary Equilibrium.

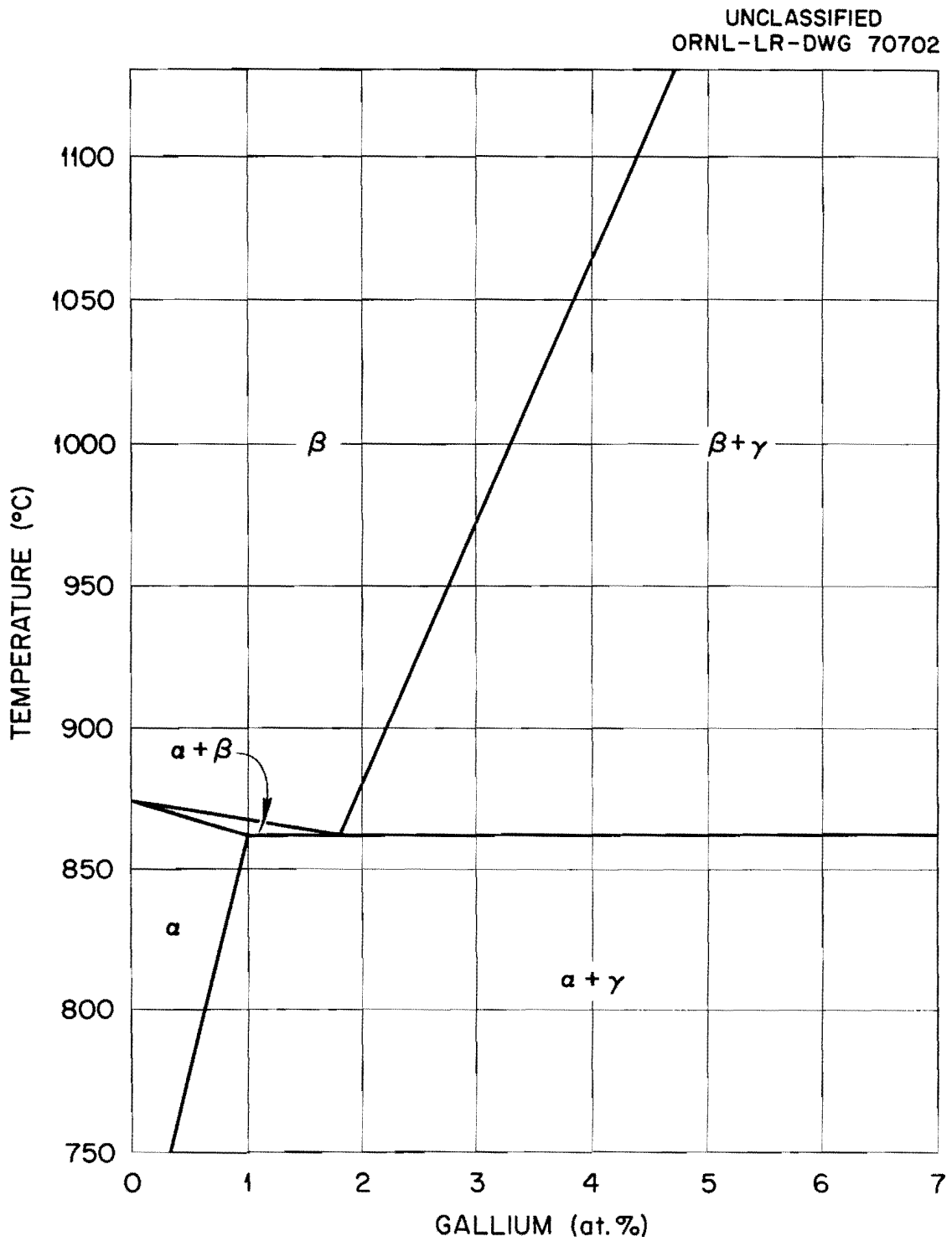

Fig. 21. Idealized Diagram of the Zr-Ga Eutectoid Region.

impurities are alpha stabilizers, then this may not be the case. However, experience has shown that the upper temperature limit of the transformation range which would be increased by this type impurity has been shown to be rather constant when measured over a period of years in the laboratory. In contrast, the lower limit has fluctuated over a wide range of temperatures depending upon the impurity level.

The beta-alpha plus beta and alpha-alpha plus beta boundaries are slightly depressed by the addition of gallium in contrast to other Group IIIB elements, aluminum[12] and indium,[13] which are alpha stabilizers as shown previously in Fig. 3. The slopes of the alpha-beta boundaries of other zirconium systems are found to correlate fairly well with the valency of the solute. The beta-alpha plus beta and alpha-alpha plus beta slopes of silver,[14] cadmium,[15] indium,[13] tin,[16] and antimony[13] have been shown previously in Fig. 2. If the average $\left(\frac{dt/dx[\alpha/\alpha + \beta] + dt/dx[\beta/\alpha + \beta]}{2}\right)$ of these slopes are plotted along with that of zirconium-gallium, as in Fig. 22, the gallium does not fit. This shift of the alpha-beta boundaries to a eutectoid type may be explained by the large size factor involved (−21%) which is unfavorable when compared to that of Al(−8%) and In(+5%).

Another indication of a large effect of gallium is the hardness increase in the transformed beta phase with the addition of gallium. The Vickers hardness number increases for various solutes at 1 at. % are: Ag-33, Cd-8, In-12, Pb-20, Sb-28, and Ga-37.[17] This would be another indication of a large size factor if one assumes hardness and size distortion of the alloy are closely related.

---

[12] D. J. McPherson and M. Hansen, Trans. ASM 46, 354–71 (1954).

[13] J. O. Betterton, Jr., J. H Frye, Jr., and D. S. Easton, Phase Diagram Studies of Zirconium with Silver, Indium, and Antimony, ORNL-2344 (Aug. 12, 1959).

[14] J. O. Betterton, Jr., and D. S. Easton, Trans. AIME, 470–75 (Aug. 1958).

[15] Met. Div. Ann. Prog. Rep. July 1, 1960, ORNL-2988, p. 123.

[16] D. J. McPherson and M. Hansen, Trans. ASM 45, 915–31 (1953).

[17] Met. Div. Ann. Prog. Rep. Oct. 10, 1958, ORNL-2632, p. 17.

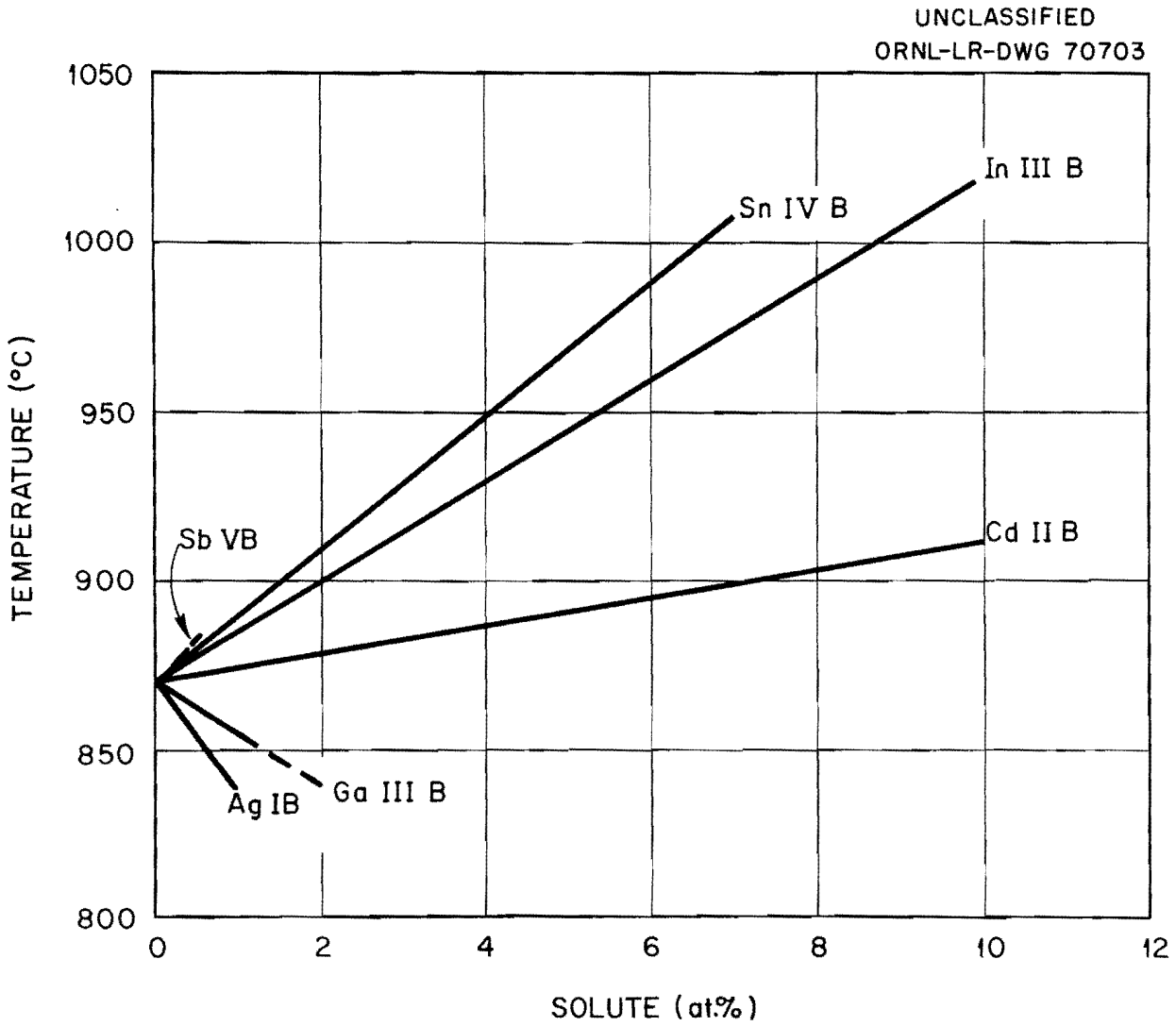

Fig. 22. Average of the Slopes of β-$\alpha + \beta$ and α-$\alpha + \beta$ Boundaries with Solutes of Varying Valencies.

The solubility of gallium in the beta phase was found to be about one third that of the aluminum and indium systems. The beta solubility limit of between 4 and 5 at. % Ga, as determined at 1100°C by bracketing the boundary, was in good agreement with a lineal analysis of the beta and gamma phases present in alloys annealed at 1095°C in the composition range of 5–16% Ga. The volume percent of the gamma phase present in these alloys (see Fig. 8) showed that the beta composition of 4.5 at. % Ga was in equilibrium with Zr_3Ga of 27 at. % Ga. The differences in these values and those shown on the phase diagram are within experimental limitations. Another series of alloys annealed at 920°C showed the same compound to be in equilibrium with beta containing 2.5 at. % Ga.

Intermediate Compounds

Alloys of 25, 29, 33.2, and 37.5 at. % Ga were examined in the as-cast condition. The 25, 29, and 33.2 at. % alloys consisted of primary crystals of a compound surrounded by a eutectic structure. Lineal analysis (along with previous samples up to 16 at. %) indicated a eutectic reaction, liquid (21.0 at. % Ga) $\leftrightarrows$ beta (8.0 at. % Ga) + Zr_5Ga_3 (37.5 at. % Ga), with the Zr_3Ga phase forming peritectoidally at some lower temperature (not determined). The 37.5 at. % alloy consisted of a matrix of Zr_5Ga_3, primary crystals of a new phase, and a small amount of eutectic. A volume percent calculation placed the composition of the primary phase at 50 at. % Ga (ZrGa). The presence of both the zirconium-gallium phase and the eutectic structure in the microstructure would suggest that Zr_5Ga_3 is an incongruently melting compound. A hypothetical diagram is shown in Fig. 23 with no temperatures indicated since they were not determined for the entire composition range.

Lattice Parameter Measurements

Lattice spacings were measured on two alloys (0.39 and 0.6 at. % Ga) which were annealed in the alpha phase region. The results, along with

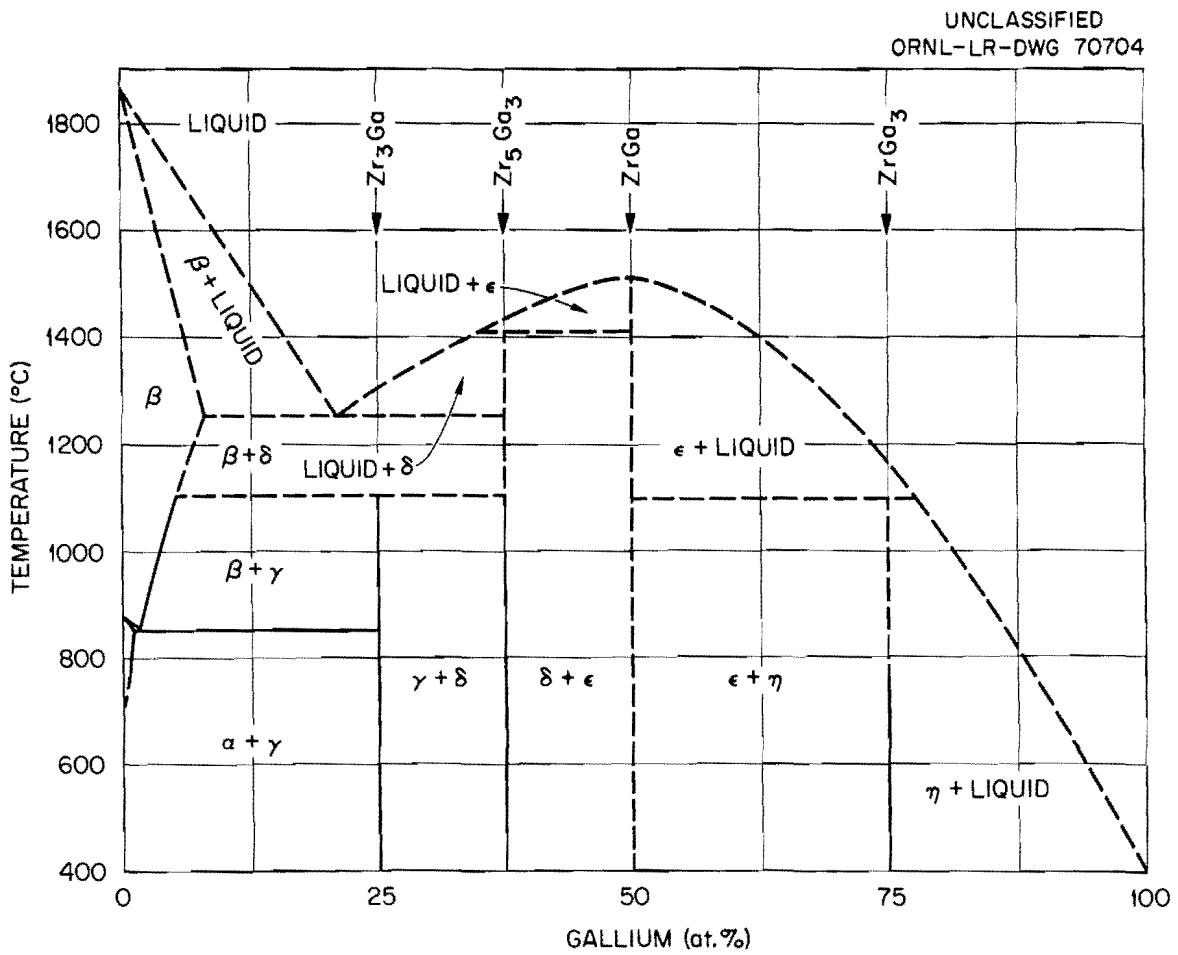

Fig. 23. Hypothetical Phase Diagram of the Zr-Ga System.

pure zirconium, are shown in Fig. 24. A discussion[18] of the effect of solute valency on parameters of various zirconium systems has shown that the proportionality of the axial ratio to solute valency was principally due to the dependence of the "c_o" spacing with the "a_o" lattice constants sharing a common slope. The changes in axial ratio of various solutes are shown plotted against the valency of the solute in Fig. 25. Gallium fits quite well, indicating that the size misfit does not have much effect on the axial ratio.

SUMMARY AND CONCLUSIONS

The zirconium-gallium phase diagram was determined primarily in the zirconium-rich region on the basis of metallographic examination of isothermally annealed samples. Intermediate phase positions were determined by examination of as-cast structures and by lineal analysis. The control of purity levels and temperatures of anneals were held to tolerances as close as possible. Materials used in the experiment were selected on the basis of purity and were as pure as available at the present time with the exception of zone-refined metal.

The results of the experiment show that gallium does not fit the same model as other Group III elements when alloyed with zirconium. The deviations may be explained by the large atomic size difference in zirconium and gallium.

The important features of the system are as follows:

1. The maximum solubility of the alpha phase was 0.8 at. % Ga at 840°C.

2. The maximum solubility of the beta phase was approximately 8.0 at. % Ga with the temperature not determined but above 1100°C.

---

[18] J. O. Betterton, Jr., and D. S. Easton, "Lattice Constants of Alpha-Zirconium Alloys with Additions of Ag, Cd, In, Sn, and Sb," paper presented at 1961 Annual Meeting of AIME, St. Louis, Mo., Feb. 26, 1961. Abstract published in J. Metals 13, 86 (1961).

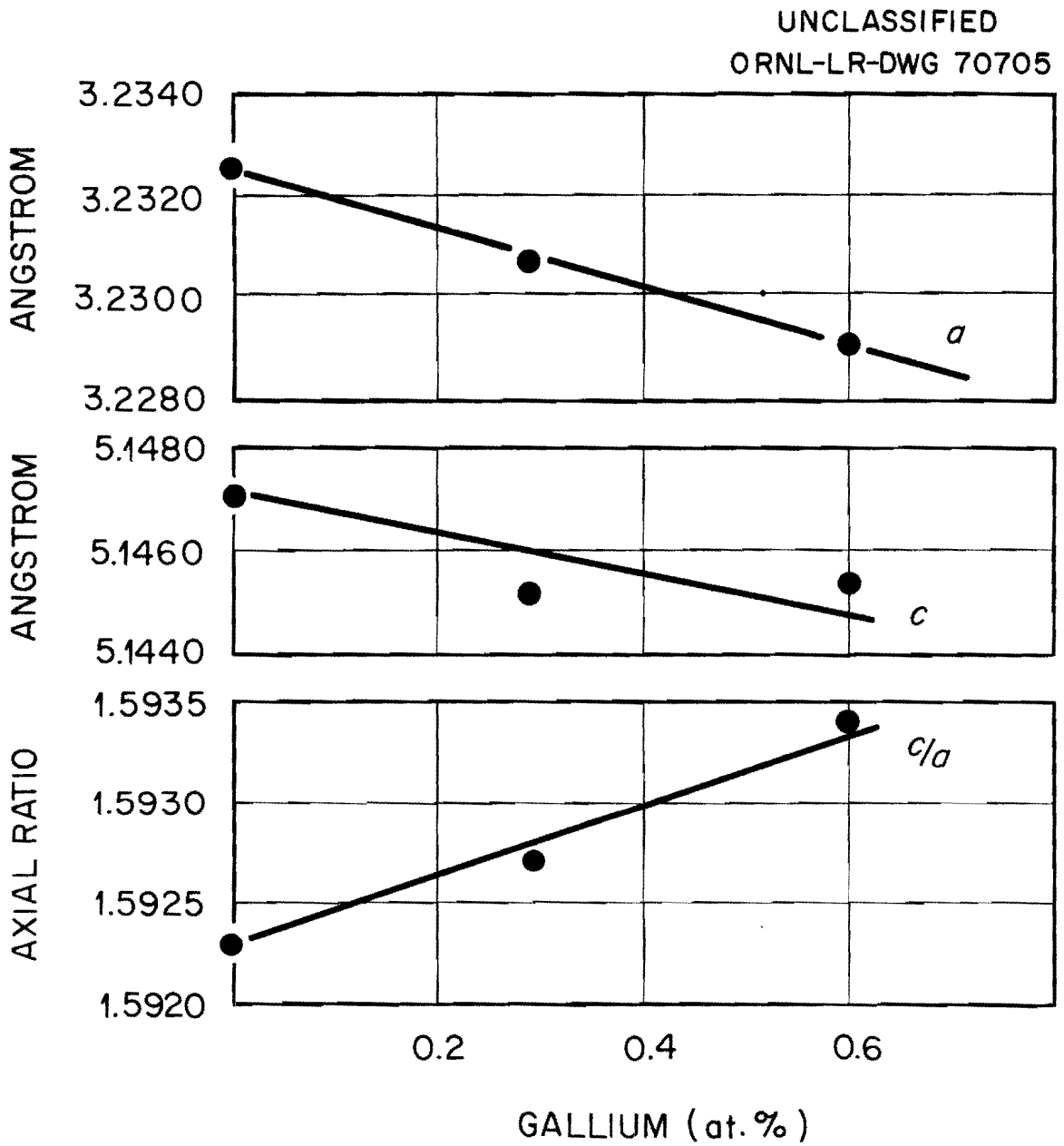

Fig. 24. Lattice Parameter Measurements in the Alpha Phase Region.

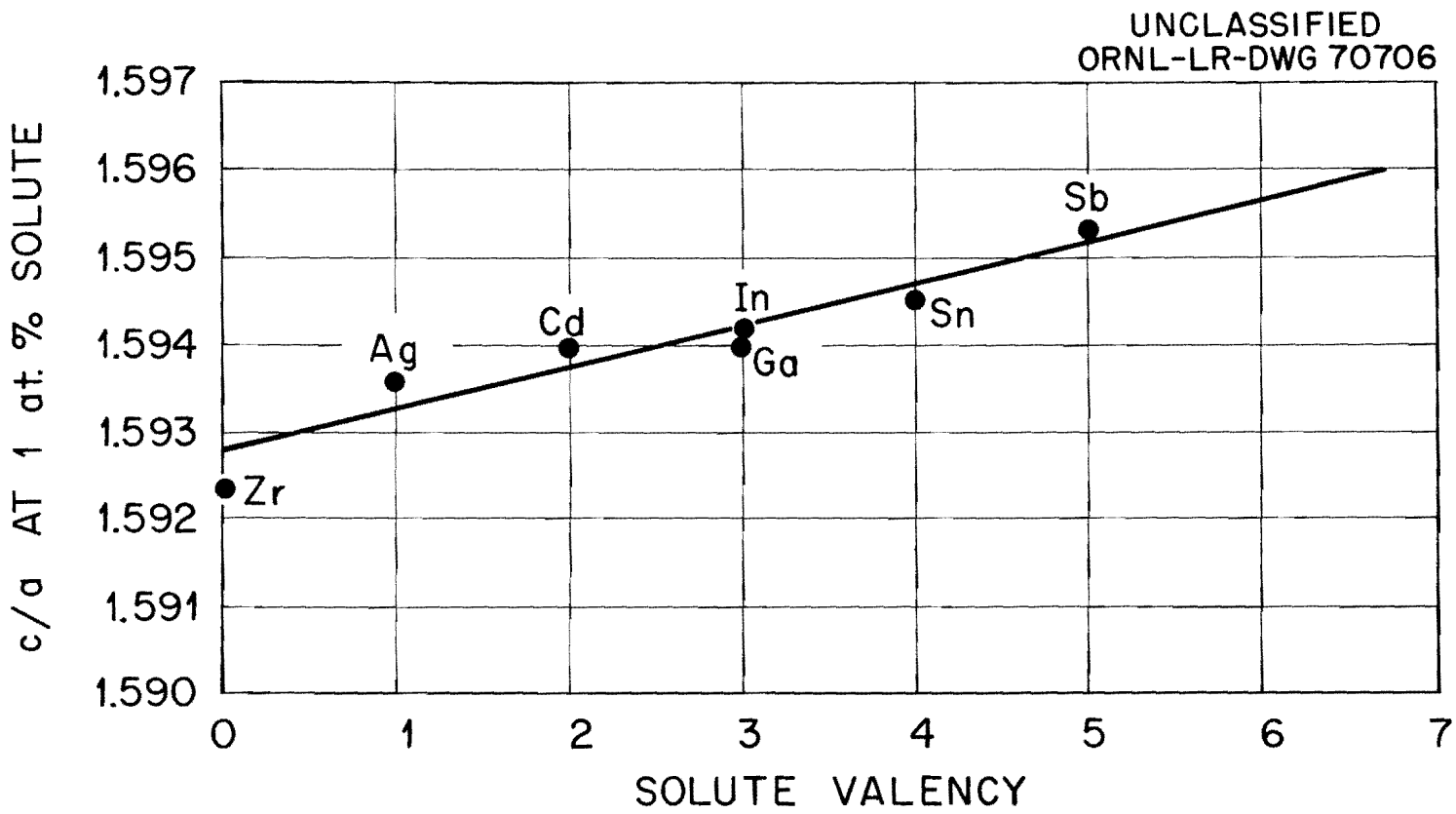

Fig. 25. Changes in Axial Ratios of Zirconium Alloys with Solutes of Varying Valency.

3. A eutectoid reaction occurred at 860°C with beta (1.8 at. % Ga) decomposing into alpha (0.8 at. % Ga) and gamma (Zr_3Ga) (25.0 at. % Ga).

4. A eutectic reaction occurred at an unknown temperature; liquid (21.0 at. % Ga) decomposing into beta (8.0 at. % Ga) and Zr_5Ga_3 (37.5 at. % Ga).

5. A compound, Zr_3Ga (25.0 at. % Ga), formed peritectoidly from beta and Zr_5Ga_3 at some temperature above 1100°C.

6. A compound, Zr_5Ga_3 (37.5 at. % Ga), formed peritectically from liquid and ZrGa at some temperature above 1100°C.

7. It is proposed that a compound, ZrGa (50.0 at. % Ga), exists. Proposed diagrams of the final results are shown in Figs. 20 and 22.

ACKNOWLEDGMENT

The author wishes to express his appreciation to J. O. Betterton, Jr., whose encouragement and leadership made this experiment possible. Gratitude is also extended to D. L. McElroy, D. A. Douglas, and other members of the Technical Qualification Committee for their consideration and advice.

APPENDIX A

Table A.1. Zirconium-Gallium Annealing Data

Sample	Arc Casting	Preliminary Anneals days	Preliminary Anneals °C	Isothermal Final Anneals days	Isothermal Final Anneals °C	Estimated Composition (at. % Ga)	Analyzed Composition (at. % Ga)	Quenched Hardness VHN	Microstructure
ZGa0.2E	6x	10	1101.0 ± 3			0.2		80.5	
				24	866.3 ± 0.4	0.2		68.9	α + β
				30	871.6 ± 0.3	0.2	0.21	96.3	α + β, ~25% α
				65	750.6 ± 0.2	0.2		63.05	α
ZGa0.4E	6x	10	1101.0 ± 3			0.4		91.2	
				24	866.3 ± 0.4	0.4		84.1	α + β
				48	799.6 ± 0.4	0.4	0.42	83.1	α
				65	750.6 ± 0.2	0.4	0.391	58.3	α + compound
ZGa0.6E	6x	10	1101.0 ± 3			0.6		81.8	
				24	866.3 ± 0.4	0.6		89.1	α + β
				33	842.9 ± 0.3	0.6	0.51	85.5	α
				45	871.3 ± 0.6	0.6	0.68	105.5	β
				48	799.6 ± 0.4	0.6	0.63	87.0	α + trace compound
ZGa0.8E	6x	7	1104.6			0.8		76	
				24	866.0 ± 0.3	0.8		86.6	α + β
				33	842.9 ± 0.3	0.8	0.755	109.5	α + β
				44	829.9 ± 0.2	0.8	0.79	99.8	α + trace compound
				48	799.6 ± 0.4	0.8	0.84	96.2	α + compound

Table A.1 (Continued)

Sample	Arc Casting	Preliminary Anneals days	Preliminary Anneals °C	Isothermal Final Anneals days	Isothermal Final Anneals °C	Estimated Composition (at. % Ga)	Analyzed Composition (at. % Ga)	Quenched Hardness VHN	Microstructure
ZGal.OE1	6x	7	1104.6			1.0		98.5	
				24	866.0 ± 0.3	1.0	1.00	94.2	$\alpha + \beta$
				33	842.9 ± 0.3	1.0	1.08	90.9	$\alpha + \beta + \gamma$
				43	854.4 ± 0.7		1.08	121.3	Three-phase 20–25% β, 2% γ, bal α
ZGalE	6x	13	1091 ± 7			1.0		99	β
				22	920.7 ± 0.4	1.0		120	β
				22	870.3 ± 0.5	1.0	1.10	85	β
				21	849.5 ± 0.6	1.0	1.16	82.9	$\alpha + \beta + \gamma$ Three-phase ~84% α, 15% β, 1% γ
ZGal.2E	6x	7	1104.6			1.2		107.2	
				24	866.0 ± 0.3	1.2	1.24	98.4	β
				33	842.9 ± 0.3	1.2	1.28	86.3	$\alpha + \gamma$
				35	859.3 ± 0.3	1.2	1.3	100.6	$\alpha + \beta$
ZGal.4E	6x	7	1104.5 ± 1			1.4		111.9	
				24	866.0 ± 0.3	1.4	1.42	102.6	β

Table A.1 (Continued)

Sample	Arc Casting	Preliminary Anneals days	Preliminary Anneals °C	Isothermal Final Anneals days	Isothermal Final Anneals °C	Estimated Composition (at. % Ga)	Analyzed Composition (at. % Ga)	Quenched Hardness VHN	Microstructure
ZGa1.8E	6x	7	1104.5 ± 1			1.8		139.2	
				24	866.0 ± 0.3	1.8	1.80	108.6	β
ZGa2E	6x	11	1095 ± 7			2.0		148.5	β
				22	920.7 ± 0.4	2.0	2.06	144	β
				21	900.0 ± 0.3	2.0	2.46	167	β + γ <1% compound
				22	870.3 ± 0.5	2.0	2.03	136	β + γ
				21	849.5 ± 0.6	2.0	–	98	β + γ + α serrated β, small γ grains, very little α
				20	910.7 ± 0.3	2.0	1.96	147	β + trace γ
ZGa2.5E	6x	7	1104.5 ± 1			2.5		146.3	
				15	950.3 ± 0.3	2.5	2.61	105.4	β
ZGa3E	6x	13	1091 ± 7			3.0		188	β
				32	985.2 ± 0.3	3.0	3.34	194	β + small amount of γ
				14	980.9 ± 0.2	3.0	3.33	203	β + trace of γ
				22	920.7 ± 0.4	3.0	2.98	151	β + ~2% compound

Table A.1 (Continued)

Sample	Arc Casting	Preliminary Anneals days	Preliminary Anneals °C	Isothermal Final Anneals days	Isothermal Final Anneals °C	Estimated Composition (at. % Ga)	Analyzed Composition (at. % Ga)	Quenched Hardness VHN	Microstructure
				22	870.3 ± 0.5	3.0	–	136	β + compound
				28	990.2 ± 0.4	3.0	3.17	196	β
ZGa4E	6x	11	1095 ± 7			4.0	4.08	218.5	β
				22	920.7 ± 0.4	4.08		160	β + γ; 6–8% γ
				5	1071.5 ± 0.3	4.08	4.4	238	β
				10	1065.4 ± 0.4	4.08	4.71	240	β + small amount γ (angular shaped)
				8	1069	4.08	4.08	205	β + trace γ
ZGa5E	6x	13	1091 ± 7			5.0		228	
				22	920.7 ± 0.4	5.0		175	β + γ
ZGa5E1	6x	13	1094 ± 4			5.0	5.08	240	β + <1% γ
				4	1130.1 ± 0.3	5.0	4.68	254	β
				4	1125.0 ± 0.7	5.0	4.79	274	β + γ; γ was generally oval shaped
ZGa6E	6x	11	1095 ± 7			5.9	6.21	274	β + γ
				22	920.7 ± 0.4	6.21		171	β + γ

Table A.1 (Continued)

Sample	Arc Casting	Preliminary Anneals days	Preliminary Anneals °C	Isothermal Final Anneals days	Isothermal Final Anneals °C	Estimated Composition (at. % Ga)	Analyzed Composition (at. % Ga)	Quenched Hardness VHN	Microstructure
ZGa7E	6x	13	1091 ± 7			7		45	Segregated
ZGa8E	6x	11	1095 ± 7			8		292	$\beta + \gamma$
ZGa9E	6x	13	1094			9		260	$\beta + \gamma$
ZGa10E	6x	10	1095 ± 10			10		286.5	$\beta + \gamma$
ZGa11E	6x	13	1094			11		268	Segregated
ZGa12E	6x	10	1095 ± 0.10			12		340.5	$\beta + \gamma$
ZGa14E	6x	12	1095 ± 10			14		325	$\beta + \gamma$ segregated
ZGa16E	6x	12	1095 ± 10			16		323.5	$\beta + \gamma$

DISTRIBUTION

1-2. Central Research Library
3. Document Reference Section
4-8. Laboratory Records
9. Laboratory Records, ORNL-RC
10. ORNL Patent Office
11. G. M. Adamson, Jr.
12. J. O. Betterton, Jr.
13. B. S. Borie
14. C. R. Boston
15. J. V. Cathcart
16. B. G. Catron
17. O. B. Cavin
18. G. W. Clark
19. J. E. Cunningham
20. D. A. Douglas
21-30. D. S. Easton
31. J. H Frye, Jr.
32. R. J. Gray
33. W. O. Harms
34-37. M. R. Hill
38. E. E. Hoffman
39. H. Inouye
40. G. D. Kneip, Jr.
41. T. S. Lundy
42. H. G. MacPherson
43. D. L. McElroy
44. C. J. McHargue
45. P. Patriarca
46. R. E. Pawel
47. G. F. Petersen
48. M. L. Picklesimer
49. R. E. Reed
50. J. L. Scott
51. G. M. Slaughter
52. G. P. Smith, Jr.
53. C. J. Sparks, Jr.
54. E. E. Stansbury
55. R. M. Steele
56. R. A. Vandermeer
57. M. S. Wechsler
58. R. O. Williams
59. H. L. Yakel
60-74. Division of Technical Information Extension (DTIE)
75. Research and Development Division (ORO)